RESEARCH ARTICLE

PM$_{10}$ source apportionment in a Swiss Alpine valley impacted by highway traffic

**Regina E. Ducret-Stich · Ming-Yi Tsai ·
Devraj Thimmaiah · Nino Künzli · Philip K. Hopke ·
Harish C. Phuleria**

Abstract Although trans-Alpine highway traffic exhaust is one of the major sources of air pollution along the highway valleys of the Alpine regions, little is known about its contribution to residential exposure and impact on respiratory health. In this paper, source-specific contributions to particulate matter with an aerodynamic diameter<10 μm (PM$_{10}$) and their spatio-temporal distribution were determined for later use in a pediatric asthma panel study in an Alpine village. PM$_{10}$ sources were identified by positive matrix factorization using chemical trace elements, elemental, and organic carbon from daily PM$_{10}$ filters collected between November 2007 and June 2009 at seven locations within the village. Of the nine sources identified, four were directly road traffic-related: traffic exhaust, road dust, tire and brake wear, and road salt contributing 16 %, 8 %, 1 %, and 2 % to annual PM$_{10}$ concentrations, respectively. They showed a clear dependence with distance to highway. Additional contributions were identified from secondary particles (27 %), biomass burning (18 %), railway (11 %), and mineral dust including a local construction site (13 %). Comparing these source contributions with known source-specific biomarkers (e.g., levoglucosan, nitro-polycyclic aromatic hydrocarbons) showed high agreement with biomass burning, moderate with secondary particles (in winter), and lowest agreement with traffic exhaust.

Keywords Source apportionment · PMF · Highway traffic · PM10 · Swiss Alpine valley · Levoglucosan · NitroPAH

R. E. Ducret-Stich (✉) · M.-Y. Tsai · D. Thimmaiah · N. Künzli ·
H. C. Phuleria
Department of Epidemiology and Public Health, Swiss Tropical and Public Health Institute, Socinsstrasse 57, P.O. Box, 4002, Basel, Switzerland
e-mail: regina.ducret@unibas.ch

R. E. Ducret-Stich · M.-Y. Tsai · N. Künzli · H. C. Phuleria
University of Basel, Petersplatz 1,
4003 Basel, Switzerland

M.-Y. Tsai
Department of Environmental and Occupational Health Sciences, University of Washington, Box 357234, Seattle, WA 98195, USA

P. K. Hopke
Department of Chemical and Biomolecular Engineering and Center for Air Resources Engineering and Science, Clarkson University, Box 5708, Potsdam, NY 13699-5708, USA

Introduction

Inhalable particulate matter consists of a complex mixture of particles and droplets of varying size and composition. They originate from different natural and anthropogenic sources, e.g., fires, windblown dust, motor vehicles, power plants, construction activities, and contain primary and secondary particles (Seinfeld and Pandis 2006). Although there is considerable evidence that airborne particulate matter (PM) is associated with adverse respiratory and cardiovascular health effects (Davidson et al. 2005; Pope and Dockery 2006; Russell and Brunekreef 2009; US EPA 2009), only few studies have examined association of apportioned components and sources of PM with health outcomes (Stanek et al. 2011).

From a policy point of view, it is crucial to identify air pollution sources that have the greatest impact on public health in order to apply targeted emission management

strategies. For example, emission regulations are continuously tightened for traffic exhaust, one of the most investigated sources (Brugge et al. 2007; Health Effects Institute 2010). However, there is increasing evidence of health impacts from other sources such as biomass burning (Laumbach and Kipen 2012; Naeher et al. 2007) or Saharan dust events (Karanasiou et al. 2012). Therefore, application of receptor modeling has become more and more important in recent years for estimating the exposure from the different sources (Hopke 2003; Viana et al. 2008).

Due to health concerns raised in communities along the main north–south transit route crossing the Alps (Hazenkamp-von Arx et al. 2011), Swiss Federal Office for the Environment funded this pediatric asthma panel study to investigate the health impact of short-term air pollution from local sources. The primary north–south transit corridor study (Hazenkamp-von Arx et al. 2011) comprised of ten communities along the Swiss Alpine highway corridors including Erstfeld, a village located in a narrow and flat Alpine valley bordered by steep mountain slopes along the Swiss transit highway A2. The focus of the current study is the chemical composition of PM in this village. One and a half years of air pollution measurements, at several sites within the village, were used to analyze the temporal and spatial distribution of the different pollutants (Ducret-Stich et al. 2013). Traffic-related pollutants such as nitrogen dioxide (NO_2), elemental carbon (EC) and particle number concentration were highly heterogeneous in space (i.e., decreasing concentrations with increasing distance to the highway). In contrast, particulate matter with an aerodynamic diameter<10 μm (PM_{10}) and organic carbon (OC) influenced also by sources other than traffic, showed a more homogeneous spatial distribution.

The aim of this paper is to find and apportion the main sources contributing to the total PM_{10} in Erstfeld using positive matrix factorization (PMF). Single sources such as traffic exhaust, biomass burning, and secondary pollutants are validated by comparison with source-specific biomarkers (e.g., levoglucosan, nitro-polycyclic aromatic hydrocarbons). We describe the spatial and temporal distribution of the source-specific contributions, with special focus on highway-related sources. The modeled source-specific contribution estimates are subsequently being used to assess acute respiratory health effects in school children.

Methods

Study description

From November 2007 to June 2009, several air pollutants were measured in Erstfeld, a village with about 3,800 inhabitants located in an 800 to 900 m wide Alpine valley in Switzerland. A detailed description of the study region, monitoring sites, and measured pollutants can be found elsewhere (Ducret-Stich et al. 2013). Daily PM_{10} filters were concurrently collected at one fixed highway and one mobile station, which was moved each month to one of the seven locations (Fig. 1). The highway site was situated north of the village right beside the highway (22 m from the centerline). From that location, three mobile sites were additionally located at perpendicular distances of 55, 102, and 198 m to the highway (Fig. 1, sites 1–3). The other four mobile sites were chosen to represent the residential area and to capture the impact of additional sources such as the main road and railways (Fig. 1, sites 4–7). The mobile station measurements were scheduled to cover all seasons for each mobile station in the residential area during the
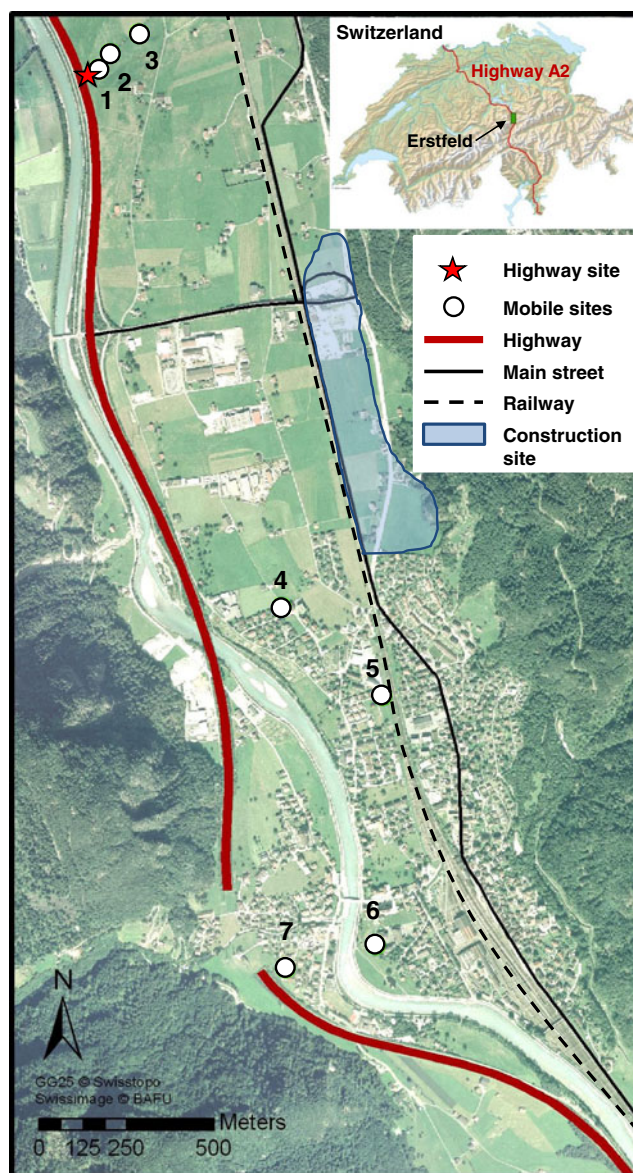

Fig. 1 Map of Erstfeld with measurement sites

study. During the whole study period there was a major construction site north-east of site 4 (Fig. 1), where the largest train tunnel in the world, the base tunnel through the Gotthard mountain (Alp Transit), is still being built.

Sampling methods

At the highway and mobile sites, high volume samplers (Digitel DHA-80) with a flow rate of 30 m³/h were used to collect concurrent 24-h PM_{10} on 150 mm quartz fiber filters (Pallflex Tissuquartz 2500QAT-UP, Pall AG, Switzerland). At the mobile sites, 24-h PM_{10} was additionally collected on 47 mm Teflon filters (PTFE 2.0 μm pore size, Blanc-Labo S.A., Switzerland) using a Partisol low volume sampler (Partisol®-Plus Modell 2025 Sequential Air Sampler, Thermo Fisher Scientific) with a flow rate of 1 m³/h. All filters were pre-weighted and pre-conditioned (48 h at 22 °C and 50 % RH), and their mass concentrations were determined by standard gravimetric methods. The limit of detection, determined as three times the standard deviation of the field blanks, was 2.3 μg/m³ (N=57) and 2.4 μg/m³ (N=30) for the quartz- and Teflon-filters, respectively. The two measurement methods (high volume versus Partisol) agreed very well with an R^2 of 0.93 (slope=0.96; intercept=−1.78 μg/m³) and a mean difference of 1.12± 2.86 μg/m³ (N=521).

Chemical analysis

All of the quartz fiber filters were analyzed for EC and OC using a thermal–optical transmission method (TOT, OCEC Analyzer Sunset Laboratory Inc.). Due to a protocol change in 2009, the filters were analyzed with two different temperature profiles. Filters from 2007/2008 were analyzed with the NIOSH700⁺ protocol, while filters from 2009 were analyzed with the EUSAAR2 protocol, details of the protocols are described separately (Ducret-Stich et al. 2013). Since the two protocols provided different EC–OC fractions, it was not possible to use the fractionated EC–OC data without losing a substantial portion of the data (>30 % corresponding to 2009 measurements). Thus, we used total EC and OC and adjusted the NIOSH700+ concentrations to levels of the EUSAAR2 protocol with the following factors derived from orthogonal regression analysis of 102 ambient filters analyzed with both protocols (Ducret-Stich et al. 2013):

$$EC_{EUSAAR2} = 1.10 \times EC_{NIOSH700+} \quad (1)$$

$$OC_{EUSAAR2} = 0.92 \times OC_{NIOSH700+} \quad (2)$$

The Teflon filters at the mobile sites were used to determine concentrations of 48 chemical elements (Table 1 and

Table 1 Summary statistics, method detection limit (MDL), % of data below MDL, signal-to-noise ratio (S/N), and PMF category of all species which were used for PMF analysis (N=510)

Species	Mean (ng/m³)	SD (ng/m³)	MDL (ng/m³)	% below MDL	S/N	PMF category
PM_{10}	15,490	9,732	2,400	0	0.8	Weak
MM[a]	3,030	3,944			0.7	Weak
EC	1,112	706	51	1	3.0	Strong
OC	2,761	1,587	476	2	2.1	Strong
Al	132	232	1.63	5	25.9	Strong
Ba	5.98	7.21	0.77	25	2.4	Weak
Br	1.77	1.07	0.29	4	8.3	Weak
Ca	340	319	0.48	0	26.3	Strong
Cl	85	172	1.73	44	25.5	Strong
Cr	3.86	3.76	0.34	3	11.9	Strong
Cu	12	10	0.43	0	20.3	Weak
Fe	975	1,024	0.48	0	26.6	Strong
K	352	281	1.10	0	26.4	Strong
Mg	32	51	2.02	22	10.4	Strong
Mn	13	11	0.43	0	20.9	Strong
Na	24	55	7.82	75	5.6	Weak
Ni	0.65	0.74	0.34	45	2.8	Strong
Pb	4.75	4.65	0.48	9	12.3	Weak
Rb	1.04	0.79	0.34	19	3.8	Strong
S	606	457	0.53	0	27.1	Strong
Si	442	625	1.20	0	26.9	Strong
Ti	14	21	0.29	3	19.1	Strong
V	0.60	0.69	0.29	42	1.4	Weak
Zn	21	15	0.58	0	22.6	Strong

For summary of all other species see Online Resource Table S1
[a] Missing mass

Online Resource Table S1) by energy-dispersive X-ray fluorescence (XRF) (Cooper Environmental Services LLC, Portland, OR, USA). After the non-destructive XRF analysis, PM was extracted from the filters using Dichloromethane (CH_2Cl_2) (Miller-Schulze et al. 2010) and combined into 1- and 2-week composites for analysis of three nitro-polycyclic aromatic hydrocarbons (NPAHs) and levoglucosan (LG), respectively. NPAHs were analyzed with two-dimensional high-performance liquid chromatography tandem mass spectrometry (Miller-Schulze et al. 2010) and included 1-nitropyrene (1-NP), a diesel marker (Albinet et al. 2007; Ringuet et al. 2012b; Scheepers et al. 1995), and 2-nitropyrene (2-NP) and 2-nitrofluoranthene (2-NFl), two markers for secondary pollution (Arey et al. 1967; Ringuet et al. 2012a, b; Sweetman et al. 1967). The wood smoke marker LG (Jordan et al. 2006; Simoneit et al. 1999) was analyzed by gas chromatography/mass spectrometry as described in Simpson et al. (2004).

Mass closure

A mass closure analysis was performed on the data by comparing the reconstructed mass (RCM) with the measured mass. To calculate the RCM, the following estimates were used:

$$OM = 1.6[OC] \tag{3}$$

$$Sulfate = 4.125[S] \tag{4}$$

$$Mineral\ dust = 2.14[Si] + 1.89[Al] + 1.66[Mg]$$
$$+ 1.40[Ca_{geo}] + 1.21[K_{geo}]$$
$$+ 1.43[Fe_{geo}] \tag{5}$$

$$RCM = [EC] + OM + Sulfate + Mineral\ dust$$
$$+ \sum anthropogenic\ part\ of\ Ca, K, Fe \tag{6}$$
$$+ \sum all\ other\ species$$

where [ ] represent the concentration of the specific element. Organic matter (OM) (Eq. 3) is accounting for the mass of oxygen and other unmeasured elements in non-carbon organic matter (Turpin and Lim 2001). Although Turpin and Lim recommended a multiplication factor larger than 1.6 for non-urban areas, we used 1.6 because of the impact from the highway traffic on the air pollution in this valley (Ducret-Stich et al. 2013). In Eq. 4, the ratio of the atomic weights of ammonium sulfate ((NH_4)$_2SO_4$) and Sulfur (S) is used assuming all the sulfate is fully neutralized and occurs on the Teflon filter as ammonium sulfate. For mineral dust (Eq. 5), the elements are assumed to be present as oxides (Chow et al. 1994). However, as anthropogenic sources also emit calcium (Ca), potassium (K), and iron (Fe), only the geogenic part of these elements were used, i.e., Ca_{geo}=1.15[Al], K_{geo}=0.61[Al], and Fe_{geo}=1.13[Al] (Gianini et al. 2012b).

RCM, as defined in Eq. 6, explained on average 76 % (SD=12 %) of the measured mass (Online Resource Fig. S2). As our OM estimate (Eq. 3) was rather conservative (Turpin and Lim 2001), the missing mass (MM), defined as measured mass minus RCM, also contained the organic mass not accounted for in Eq. 6. In addition, RCM did not include nitrates, which were not measured in this study. Because MM showed higher concentrations in winter, MM was assumed to represent nitrates, which are mostly present as ammonium nitrate (NH_4NO_3) and readily form and persist in cold temperature environments (Seinfeld and Pandis 2006). MM, with an average of 24 % PM_{10} mass, was also comparable to secondary nitrate contributions to PM_{10} in other Swiss

regions (22–32 %) (Gianini et al. 2012a). Therefore, we included the MM as an additional "species" representing nitrates and additional organic matter in the source apportionment analysis.

Receptor modeling

To find and apportion the different sources of PM_{10}, we used the PMF software from the U.S. Environmental Protection Agency (EPA PMF 3.0). PMF is a receptor model, which solves a positively constrained bilinear mass balance model based on a weighted least-squares fit (Paatero 1997; Paatero and Tapper 1994).

Database construction

Chemical species with a large fraction (>50 %) of concentrations below the method detection limit (MDL) were excluded from the analysis (Online Resource Table S1), except sodium (Na), which was included as a tracer for road salt. Arsenic (As) was excluded due to weak signals where only 31 % of the concentrations were above three times the MDL. Most species with an atomic number above 40 (zirconium (Zr)) except for lead (Pb), and barium (Ba) were excluded because of the difficulties in XRF analysis. Phosphorus (P) was also excluded as it is generally a poor variable in XRF analysis due to the influence of the large Sulfur (S) peak that is adjacent in the X-ray spectrum. The final data included 24 species (Table 1).

Concentrations and uncertainties of the chemical species data were processed according to Polissar et al. (1998) for the PMF analysis. Values below the MDL were replaced by half of the MDL values, and their uncertainties were set to 5/6 of the MDL values. There were no missing values in our data set. For EC and OC, the uncertainties were set to the sum of ½ of the minimum measured value of all samples (EC, 0.01 μg/m^3; OC, 0.12 μg/m^3) plus instrument detection limit obtained from the manufacturer (0.04 μg/m^3) plus MDL, defined as three times the standard deviation of the field blanks calculated for each set of blanks (2007/2008 data (NIOSH700+) and 2009 data (EUSAAR2)) (e-CFR, 2012). The uncertainty in the MM was calculated as the square root of the sum of the variances of all measured species and measured mass (Wu et al. 2007). PM_{10} was additionally included as an independent variable into the PMF model to directly obtain the source contributions to the daily PM_{10} mass concentrations. It is assigned a high uncertainty of four times the value to decrease its weight in the model fit (Kim et al. 2003b). Uncertainty of species with a signal-to-noise ratio (S/N)<2 (PM_{10}, MM, vanadium (V)) were increased by a factor of three by categorizing them as "weak" in the PMF analysis (Norris et al. 2008; Paatero and Hopke 2003). Also Na, Ba, and Pb were set to weak to

account for their poor data quality described above. In addition, bromine (Br) and copper (Cu) were categorized as weak to reduce the number of scaled residuals$>\pm3$ (Norris et al. 2008; Paatero and Hopke 2003).

Unusual events can distort the results of source profiles and contributions (Norris et al. 2008); therefore, 19 of 529 samples were excluded from our analysis due to: fireworks (high Ba and K, $N=3$); two Saharan dust events in May and October 2008 (high PM_{10}, silicon (Si), magnesium (Mg), aluminum (Al), titanium (Ti), $N=6$); possible local events from the construction site (high Si, Mg, Al, Ti, $N=6$); local road salt spreading (very high Na and chlorine (Cl), $N=1$); and three unexplained local events with high Pb, zinc (Zn); high Ba, K, molybdenum (Mo); and high P, respectively. Summary statistics of the final 510 samples included in the PMF analysis are provided in Table 1.

Model execution

PMF was run in the robust mode for seven to ten sources using all 510 samples together. To determine the final number of sources, the distribution of the scaled residuals was examined to ensure the data were properly fitted. The extracted profiles were compared with profiles from the literature. This combination of tests was used to identify the most physically reasonable solution. The best results were found for nine sources. For up to eight sources, the residuals were positively skewed and with ten sources the tire and brake wear factor split into two unrecognizable factors. The model uncertainty was tested with bootstrapping (100 runs) (Norris et al. 2008). All factors were mapped to a base factor in every run, indicating a stable result.

PMF does not generally produce a unique solution due to rotational ambiguity (Paatero et al. 2002). Therefore, PMF solutions were systematically explored by varying the Fpeak parameter between -1 and $+1$ to find Fpeak–intervals for which the penalty function $Q(E)$ values remained relatively constant (Norris et al. 2008; Paatero et al. 2002). For these intervals, PMF solutions were analyzed using *G space plotting* to investigate statistical dependence between source contributions caused by unrealistic rotations (Paatero et al. 2005). An Fpeak value of -0.2 was found to give the best results after comparing the *G space* plots and source profiles. For Fpeak$=0$ several profiles displayed unrealistic values as shown in Online Resource Fig. S3.

Validation of the final PMF solution was done by regressing the predicted PM_{10} (sum of all source contributions from PMF) with the measured PM_{10} which resulted in an R^2 of 0.87 (Fig. 2). However, an increasing dispersion around the regression line was observed for higher mass values measured mainly in winter (Fig. 2). This might be caused by the underestimation of the organic matter in winter and/or some loss of semi-volatile material on the filters due to temperature changes before weighing. The
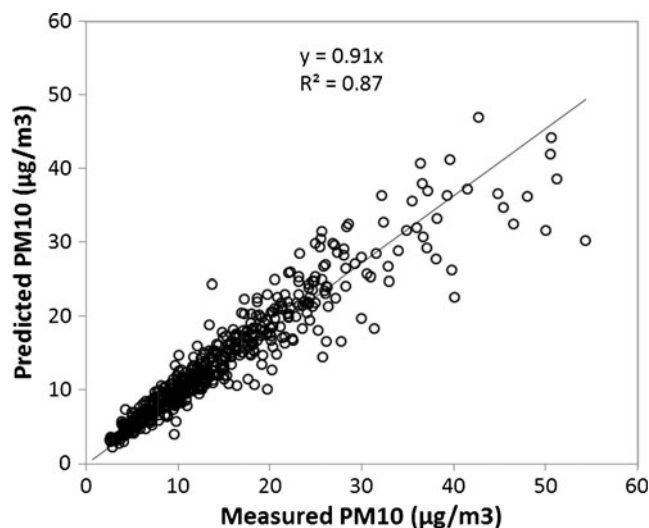

Fig. 2 Comparison of measured PM_{10} concentrations versus PMF predictions

PMF solution was additionally validated using measurements of the biomarkers levoglucosan and NPAHs to further compare source-specific contributions from biomass burning, traffic exhaust, and secondary pollution.

Results and discussion

Source profiles

We identified nine sources of which four were directly traffic-related, namely, traffic exhaust, road dust, tire and brake wear, and road salt (Fig. 3). Traffic was also indirectly related to secondary particles by producing some of their precursors. Other sources were biomass burning, railway, and two mineral-related sources, mineral dust, and minerals from the construction site (Fig. 4).

Traffic exhaust

The traffic exhaust profile was dominated by EC and OC with some contributions of abrasion-related metals such as Zn, Ba, and Cu (Schauer et al. 2006) (Fig. 3a). Source contributions were higher on weekdays than on weekends. This result corresponded to the higher weekday traffic counts of heavy duty trucks (with lower counts on weekends due to a Sunday truck traffic ban) than to the total traffic, which showed higher counts on weekends (Ducret-Stich et al. 2013) (Online Resource Fig. S4b). Although this relationship seemed to point to a strong correlation between attributed traffic exhaust PM_{10} and diesel-powered heavy duty trucks, comparison with the diesel marker, 1-NP, showed only an R^2 of 0.13 (Fig. 5a). A higher correlation was obtained with the more general traffic marker NO_2 ($R^2=0.50$) (Fig. 5b). In contrast to daily
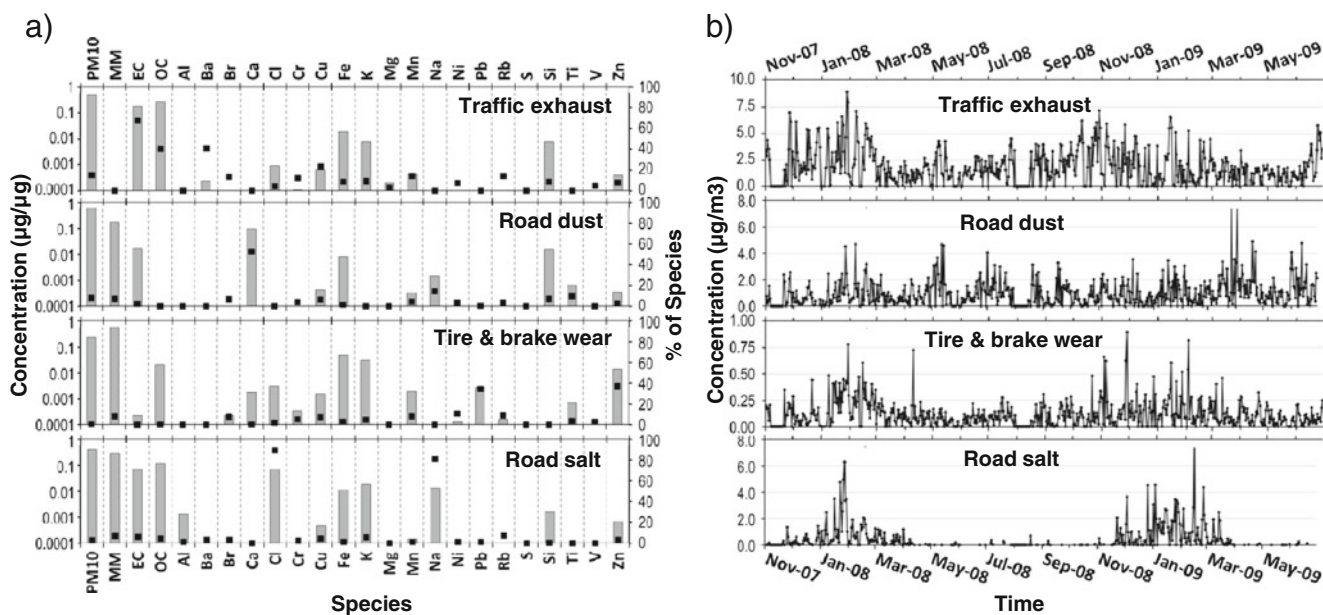
Fig. 3 Attributed sources directly related to traffic: **a** PM$_{10}$ source profiles (*solid bars, left axis*) with explained variation (*squares, right axis*) and **b** daily PM$_{10}$ source contributions. *Left axis* in source profiles describes the normed concentration such that the sum of all elemental contribution within a factor equals 1

NO$_2$ measurements, 1-NP was only available as weekly average concentrations. Moreover, filter reaction artifacts during sampling may have resulted in overestimation of 1-NP and thus to the low correlation with traffic exhaust PM$_{10}$. Reported EC/OC ratios for gasoline and diesel vehicle emissions typically range between 0.1 to 0.5 and 1.0 to 4.0, respectively (Liu et al. 2006; Lough et al. 2007). The EC/OC ratio of 0.7 in our study reflected the mixed traffic fleet with about 14 % of heavy duty vehicles (diesel) and 86 % passenger cars of which about 18 % used diesel.
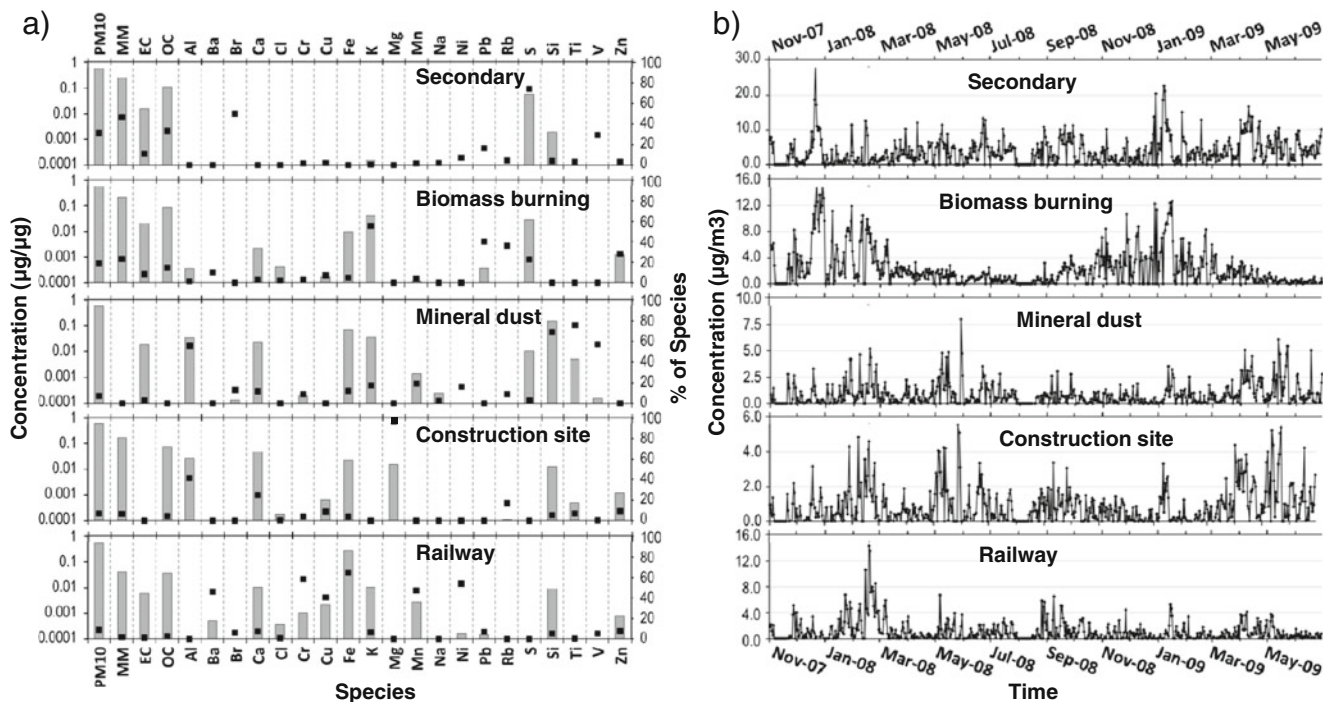

Fig. 4 Attributed sources not directly related to traffic: **a** PM$_{10}$ source profiles (*solid bars*, *left axis*) with explained variation (*squares, right axis*) and **b** daily PM$_{10}$ source contributions. *Left axis* in source profiles describes the normed concentration such that the sum of all elemental contribution within a factor equals 1
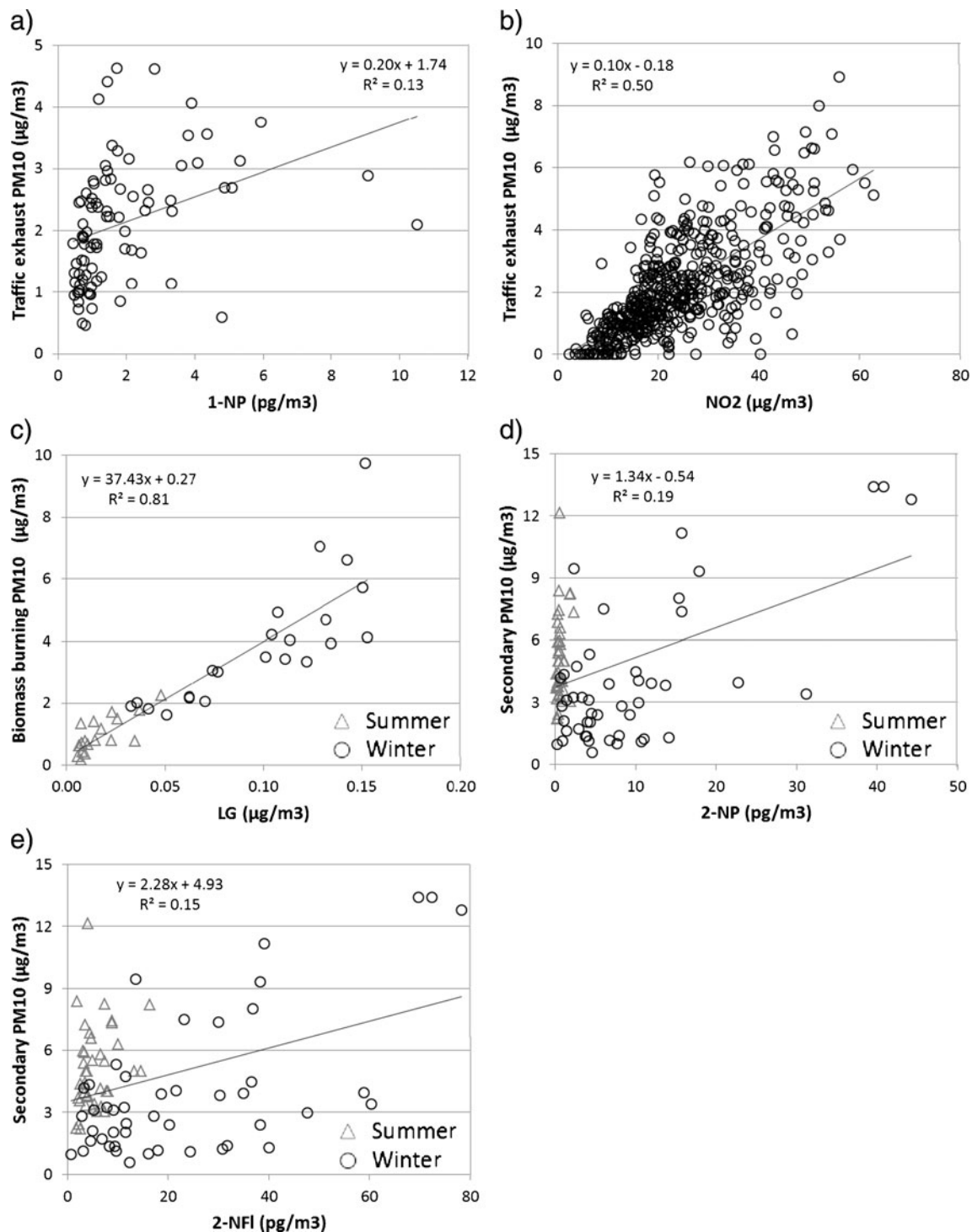
Fig. 5 Comparison of source contributions with biomarkers: traffic exhaust PM_{10} versus **a** 1-NP and **b** NO_2; **c** biomass burning PM_{10} versus levoglucosan; secondary particles versus **d** 2-NP and **e** 2-NFl. The individual regression equations correspond to all data combined

The seasonal differences with higher concentrations in winter than summer (Fig. 3b) were not related to traffic counts, which were higher in summer (Ducret-Stich et al. 2013) but rather to the meteorology. Air pollution levels were generally higher in winter than in summer due to lower wind speeds and lower mixing heights including frequent

inversions in this valley (Ducret-Stich et al. 2013). In Fig. 6, exhaust and non-exhaust (i.e., resuspended road dust, tire, and brake wear) traffic source contributions were compared between sites at different distances from the highway. For traffic exhaust, a clear gradient was observed with the higher contributions being closer to the highway.
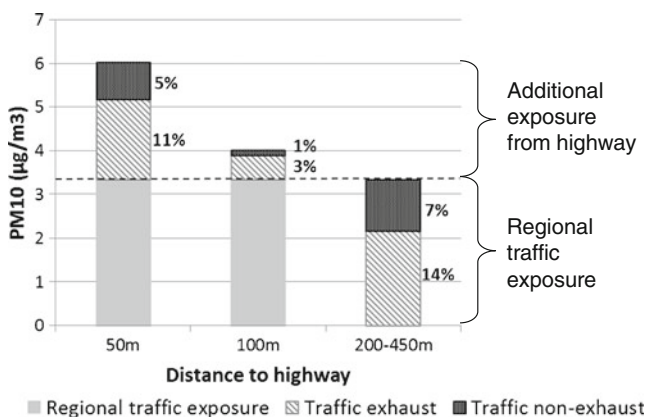
Fig. 6 Spatial distribution of traffic source contributions for the year 2008. Concentrations are normalized by the ratio of the concurrently measured PM_{10} and the annual average PM_{10} measured at the highway site. Data were averaged as follows: site 1 (50 m), site 2 (100 m), average of sites 4–6 (200–450 m). Exclusions: site 3 (only nine samples) and site 7 (protected by tunnel and noise wall)

Some recent studies have used EC and OC fractions to apportion traffic exhaust into diesel and gasoline sources (Kim and Hopke 2005; Kim and Hopke 2004; Liu et al. 2006). However, in our attempt to use EC and OC fractions in the PMF analysis, the traffic exhaust factor was not split. It must be mentioned that for the analysis with fractions, only two thirds of the data were available due to different procedures in the analysis of EC and OC (see "Chemical analysis").

Road dust

Road dust profiles are often difficult to identify due to similar elements seen in mineral dust. Our road dust profile included Si and Fe but differed from mineral dust with a high contribution of Ca (Hueglin et al. 2005; Schauer et al. 2006; Thorpe and Harrison 2008) (Fig. 3a). Contributions of this factor were higher in spring and summer (Fig. 3b), probably due to dryer weather conditions enhancing resuspension. They were also higher on weekdays, probably due to the heavy duty traffic (Online Resource Fig. S4c), which causes more resuspension of road dust than passenger cars (Bukowiecki et al. 2010; Gehrig et al. 2004).

Tire and brake wear

Tire and brake wear contributed to higher concentrations of Cu, Fe, Zn, and Pb (Bukowiecki et al. 2010; Schauer et al. 2006; Thorpe and Harrison 2008) (Fig. 3a). Concentration levels were a little elevated in winter (Fig. 3b) probably caused by higher abrasion of winter tires and increased braking due to the weather conditions. Higher concentrations were again observed on weekdays (Online Resource Fig. S4d) likely the result of heavy duty truck traffic (Bukowiecki et al. 2010).

Road salt

The de-icing road salt factor had a very clear signature with more than 80 % of Na and Cl apportioned to it (Gianini et al. 2012a) (Fig. 3a). This factor was only seen in winter (Fig. 3b) and showed no differences with respect to day of the week.

Biomass

The biomass burning profile was characterized by high concentrations of K, EC, and OC (Gianini et al. 2012b; Khalil and Rasmussen 2003; Reid et al. 2005) and other typical elements for wood smoke (Rb, S, Fe, Ca) (Godoy et al. 2005; Reid et al. 2005) (Fig. 4a). The EC/OC ratio was 0.24, which was on the upper level compared with other studies in Switzerland (Gianini et al. 2012b; Szidat et al. 2006). This somewhat higher ratio might be explained by higher contributions from EC combined with substantial amounts of Pb and Zn observed in the profile (Fig. 4a) pointing to a mixture of biomass burning with some traffic. This was supported by factor contributions in summer, when almost no biomass burning should have been present (Fig. 4b). Nevertheless, PM_{10} contribution from this biomass profile was highly correlated with the known wood biomarker levoglucosan ($R^2=0.81$, Fig. 5c). In winter, OC also showed a good correlation with biomass burning ($R^2=0.72$), whereas EC primarily originated from traffic ($R^2=0.86$) (Online Resource Fig. S5).

Secondary particles

The secondary particle factor included about 75 % of MM, 50 % of S, and about 30 % of OC (Fig. 4a). MM was assumed to represent nitrates and part of the organic matter (see "Mass closure") while S associated with OC represented sulfates in the secondary aerosol (Gianini et al. 2012a; Kim et al. 2003a). Except during two inversion episodes in December 2007 and January 2009, this factor showed generally higher contributions in spring and summer (Fig. 4b), when increased photochemical activity is favoring the formation of secondary particles (Kim et al. 2003a; Seinfeld and Pandis 2006). This result was also shown by the measured ratio between 2-nitrofluoranthene and 2-nitropyrene (2-NFl/2-NP) of 5.7 (9.0 in summer, 2.6 in winter) indicating that secondary particles were mainly formed by reaction with daytime OH– rather than NO_3-radicals (Arey et al. 1986). Nevertheless, the correlations between secondary PM_{10} and 2-NFl or 2-NP were small with an R^2 of 0.15 and 0.19, respectively (Fig. 5d, e). These results were heavily influenced by the very low concentrations of 2-NFl and 2-NP in summer showing almost no correlation with secondary PM_{10}. Correlations in winter were stronger with 0.40 and 0.49 for 2-NFl and 2-NP, respectively. In contrast to daily secondary particle contributions, nitro-PAHs were

only available as weekly concentrations leading to generally low correlations. Also, some of the nitro-PAHs may be present as a result of sampling artifacts (Schauer et al. 2003) and thereby lower the observed correlations.

Mineral factors

Contributions from mineral sources were split into two profiles: mineral dust and construction site emissions (railway tunnel "Alp Transit") (Fig. 4a). The crustal elements Si, Al, Ca, and Fe were shared by both profiles. While most of the Si was apportioned to mineral dust, almost all Mg was present in the construction site factor. Mg as an additive to the concrete, which was prepared with recycled excavated material and used on site, might have caused the PMF to apportion Mg unevenly between the two sources. The construction site factor also contained substantial amounts of Ca and Zn. These elements might be explained by the extensive use of lubricating oil for drilling machines in the tunnel as well as conveyor belts and diesel locomotives outside. Ratios of Ca/Al, K/Al, and Fe/Al for the mineral dust factor (0.64, 1.03, and 2.02, respectively) and for the construction site factor (1.80, 0.0, and 0.85, respectively) were different compared with the geogenic ratios (1.15, 0.61, and 1.13,

respectively) in northern Switzerland (Gianini et al. 2012b). However, the ratios of the two source profiles combined were again similar to the geogenic ratios with Ca/Al=1.14, K/Al=0.59, and Fe/Al=1.52. PMF was not able to clearly split these two sources, which was also reflected in the persistently observed correlations in the *G space* plots between these two factors. If additional information were available on the composition of the material from either source, then a clearer separation such as that obtained by Amato et al. (2009) might have been possible. Both mineral factors showed similar weekday patterns with peaks on Tuesdays and Thursdays (Online Resource Fig. S4e). These peaks might be driven by some activity patterns on the construction site, because all high mineral factor concentrations were measured at site 5, which was closest to the construction site. Due to the similarities of the two factors, we combined them to one total mineral dust factor for the description of contributions in "Source contributions."

Railway

The railway profile showed typical abrasion elements such as Fe, Cu, manganese (Mn), chromium (Cr), and nickel (Ni) (Bukowiecki et al. 2007) (Fig. 4a). However, Cu, Mn, and
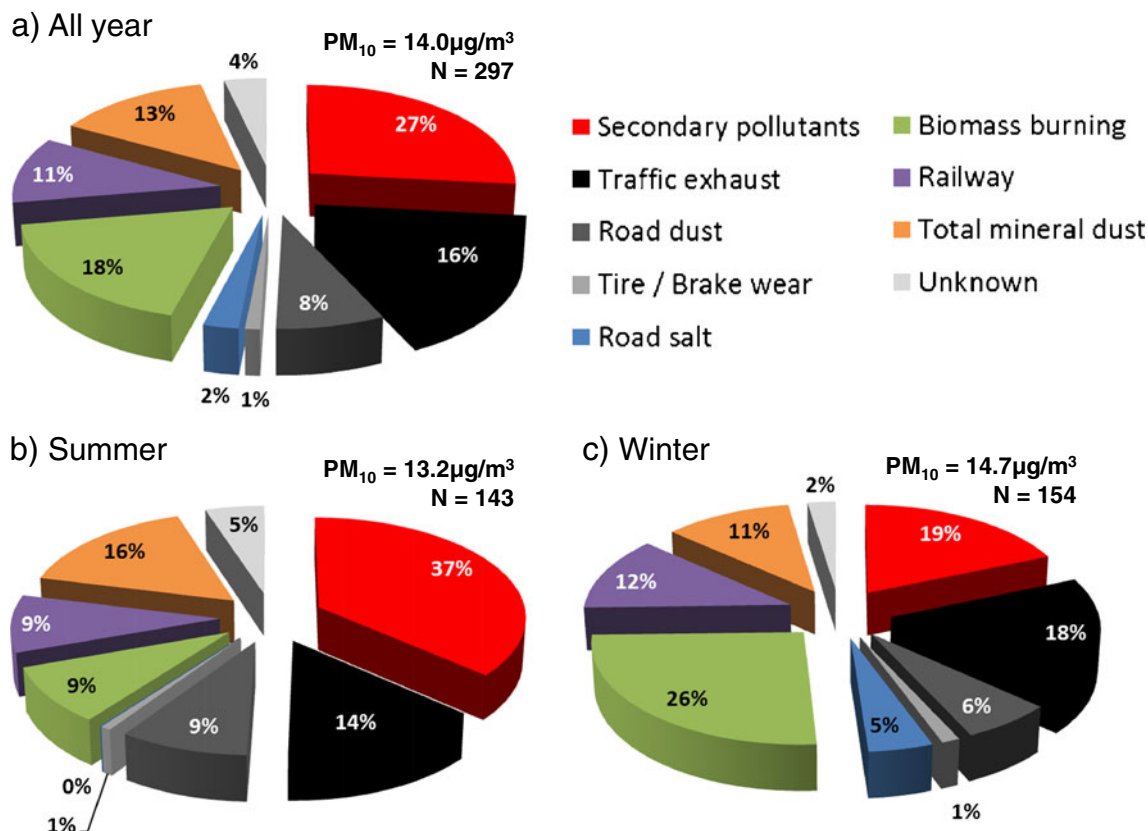

Fig. 7 Average source contributions for the year 2008: **a** the whole year, **b** in summer (Apr–Sep), and **c** in winter (Oct–Mar). Average daily PM$_{10}$ concentrations with number of measurements for the respective measurement periods are shown adjacent to the pie charts

Cr were emitted in very low quantities compared with Fe (Cu/Fe=0.01, Mn/Fe=0.01, Cr/Fe<0.005) comparable to a study in Zürich (Gehrig et al. 2007). In Switzerland, trains nearly exclusively operate with electric locomotives. However, due to the absence of power lines, diesel locomotives were used for the construction site. This presence of diesel engines might explain the additional contributions of Ba, Zn, EC, and OC in the source profile (Fig. 4a). Contributions of this factor were always highest at the site 5, which was closest to the railway tracks (Fig. 8).

Source contributions

In Fig. 7, source contributions are summarized by season for all sites in Erstfeld. To prevent over-representation of the winter months, only data from the year 2008 were used. To compare the contributions among the sites and seasons (Fig. 8), the sites closest to the highway (sites 1-3, Fig. 1) were excluded because of limited and unbalanced data in 2008 for these sites (i.e., only summer data for site 1 (N=9), only winter data for site 2 (N=32) and site 3 (N=9)). Overall, secondary pollution was the main contributor to PM_{10} in summer, while traffic and biomass burning were

more important in winter (Fig. 7). In summer, greater photochemical activity boosts the formation of secondary pollutants, while stable air masses and frequent inversions trap the pollutants in the valley in winter, increasing the importance of local sources such as traffic and biomass burning. The importance of secondary pollution in Erstfeld was also reflected in the ratio of 2-nitrofluoranthene and 1-nitropyrene (2-NFl/1-NP), which was >5 at all sites except site 1, indicating a domination of nitro-PAHs by atmospheric reactions rather than primary emissions (Miller-Schulze et al. 2010).

Although total PM_{10} concentrations were spatially homogeneously distributed (Ducret-Stich et al. 2013), large differences were observed for local traffic, railway, and mineral contributions to PM_{10} (Fig. 8). In both seasons, relative traffic source contributions were higher close to the highway (Figs. 6 and 8). At site 5, which was only 22 m away from the railway tracks and the closest measuring station to the construction site, we observed the highest contribution from the railway and mineral sources (Fig. 8).

The average PM_{10} concentration of 14.0 μg/m³ in this study was lower compared with other sites from the Swiss national air pollution monitoring network (NABEL) (Gianini
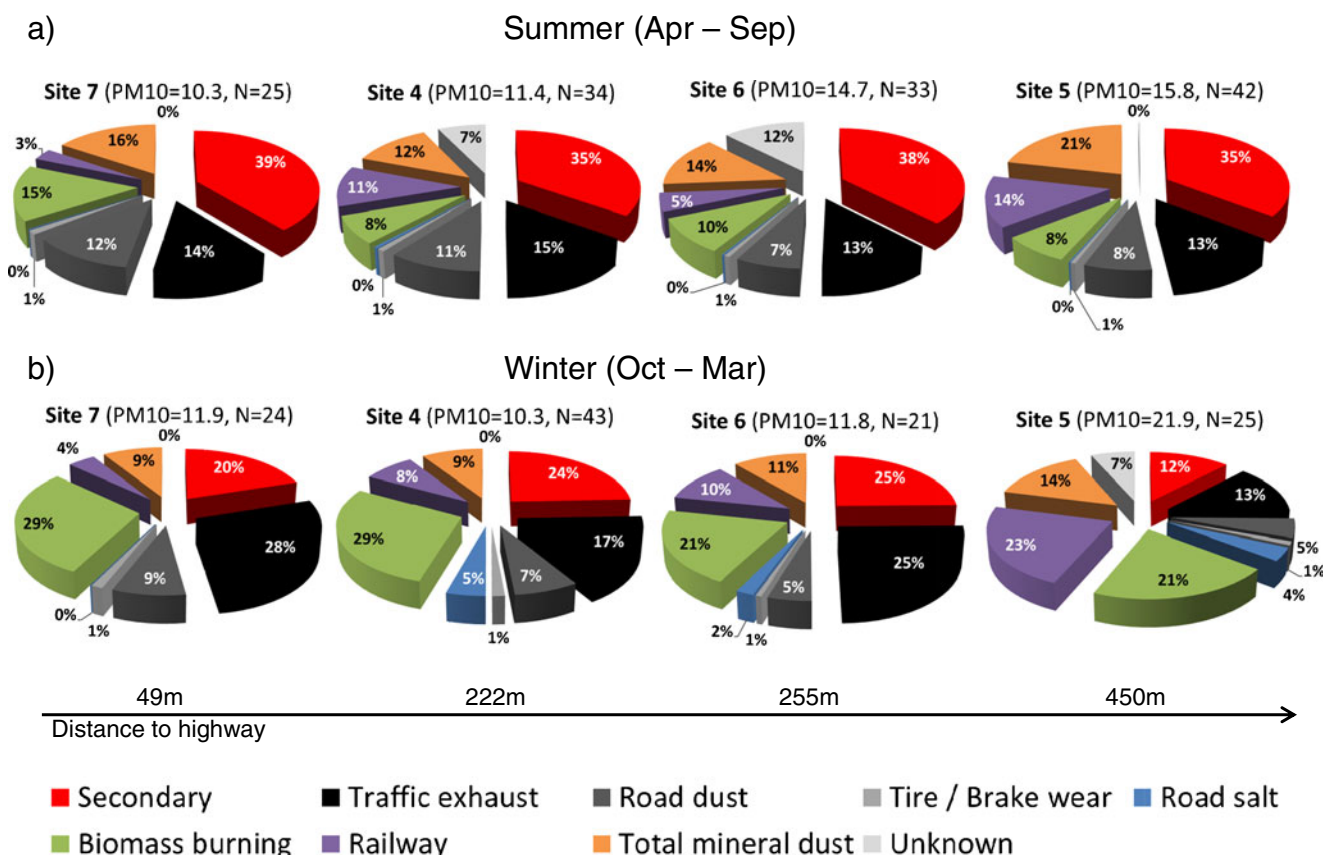

Fig. 8 Estimated source contributions by season for the four sites in the residential area for the year 2008. Site 7 is protected by a tunnel and a noise barrier from the direct influence of the highway; site 5 is closest to the railway and the construction site. Average daily PM_{10} concentrations [micrograms per cubic meter] together with number of measurements at various sites are presented in *brackets*

et al. 2012b) and comparable to other European rural background sites (Putaud et al. 2010). However, the relative contribution to PM$_{10}$ of total traffic (i.e., exhaust, road dust, tire and brake wear) was about 25 %, which was higher than in Zürich (18 %, urban background), almost as high as in Bern (30 %; urban roadside), and comparable to the rural site Magadino (24 %) south of the Alps, which is also influenced by the same highway as in our study (Gianini et al. 2012a). These results emphasize the large influence of highway traffic on the composition of particulate matter.

Secondary pollution contributions (27 %) were again comparable to Magadino (29 %) and lower than at all other NABEL sites (37–52 %) (Gianini et al. 2012a). In the European context, secondary aerosol contributions were comparable to urban sites in Central Europe (Putaud et al. 2010). This lower contribution might be a result of less photochemical activity due to the decreased sunlight in the narrow mountain valley of Erstfeld. Also, PMF might underestimate the contribution of this factor due to the lack of measurements of sulfate, nitrate, and ammonium in this study.

Another important source was biomass burning (primarily wood burning in winter). With a relative contribution of 18 %, biomass PM$_{10}$ was higher in our study than at NABEL sites (11–14 %), except for Magadino, which had a very high contribution of 31 % (Gianini et al. 2012a). In other studies, close to Magadino, it has been shown that wood burning is a major source in this region (Sandradewi et al. 2008; Szidat et al. 2007). The combination of the mountain–valley terrain, strong inversion conditions in winter, and extensive use of wood as a home heating fuel led to these high contributions to PM$_{10}$.

In Erstfeld, the construction site was probably the reason for the higher total mineral dust (i.e., mineral dust and construction site) contribution of 13 % compared with other rural sites in Central Europe (9 %) (Putaud et al. 2010) and the NABEL sites in Switzerland (8–13 %) (Gianini et al. 2012a).

As the result of having an extensive data set of daily measurements from seven different monitoring sites within the valley over one and a half years, we were able to separate different sources spatially and seasonally even though our study region was rather small. Also, additionally measured biomarkers (i.e., levoglucosan, NPAHs) allowed us to independently compare and validate some of the source contributions. However, as measurements were not concurrently collected at the different sites and no representative background measurements were available, it was not possible to compare daily contributions between the sites. The aim to distinguish between diesel and gasoline traffic sources from the highway could also not be achieved. Because of the method change in the EC and OC analysis, comparable fractionated data were only available for part of the data set. Using only the subsets, PMF was not able to give stable results.

Conclusions

In general, traffic, secondary particles from precursors of various sources—including traffic—and biomass burning were the major contributors to PM$_{10}$ in the alpine village of Erstfeld in 2008 accounting for 27 %, 27 %, and 18 % of the total PM$_{10}$ concentrations, respectively. PM$_{10}$ exposure attributed to traffic was more comparable to urban sites than those observed in rural sites in Switzerland. Also, a clear spatial dependency from the nearby highway was observed, showing increasing contributions of traffic exhaust and non-exhaust PM$_{10}$ with decreasing distance to the highway. While secondary particle contributions were lower, the biomass burning contributions were higher in Erstfeld compared with other northern Swiss villages, due to the combination of topography, winter inversions, and the importance of wood as an energy source in the Alps. However, contributions were much lower than in Magadino in the southern Alps, where biomass burning is known to be the major source of PM. The local influences of railway traffic and a major construction site were also observed. These receptor modeling results are being used to investigate the source-specific impact of air pollution exposures on short-term respiratory health outcomes in children in the village.

References

Albinet A, Leoz-Garziandia E, Budzinski H, Villenave E (2007) Polycyclic aromatic hydrocarbons (PAHs), nitrated PAHs and oxygenated PAHs in ambient air of the Marseilles area (South of France): concentrations and sources. Sci Total Environ 384:280–292. doi:10.1016/j.scitotenv.2007.04.028

Amato F, Pandolfi M, Escrig A, Querol X, Alastuey A, Pey J, Perez N, Hopke PK (2009) Quantifying road dust resuspension in urban environment by multilinear engine: a comparison with PMF2. Atmos Environ 43:2770–2780. doi:10.1016/j.atmosenv.2009.02.039

Arey J, Zielinska B, Atkinson R, Winer AM, Ramdahl T (1967) Pitts Jr JN (1986) The formation of nitro-PAH from the gas-phase reactions of fluoranthene and pyrene with the OH radical in the presence of NOx. Atmos Environ 20:2339–2345. doi:10.1016/0004-6981(86)90064-8

Brugge D, Durant J, Rioux C (2007) Near-highway pollutants in motor vehicle exhaust: a review of epidemiologic evidence of cardiac and pulmonary health risks. Environ Health 6:23. doi:10.1186/1476-069X-6-23

Bukowiecki N, Gehrig R, Hill M, Lienemann P, Zwicky CN, Buchmann B, Weingartner E, Baltensperger U (2007) Iron, manganese and copper emitted by cargo and passenger trains in Zürich (Switzerland): size-segregated mass concentrations in ambient air. Atmos Environ 41:878–889. doi:10.1016/j.atmosenv.2006.07.045

Bukowiecki N, Lienemann P, Hill M, Furger M, Richard A, Amato F, Prévôt ASH, Baltensperger U, Buchmann B, Gehrig R (2010) PM10 emission factors for non-exhaust particles generated by road traffic in an urban street canyon and along a freeway in Switzerland. Atmos Environ 44:2330–2340. doi:10.1016/j.atmosenv.2010.03.039

Chow JC, Watson JG, Fujita EM, Lu Z, Lawson DR, Ashbaugh LL (1994) Temporal and spatial variations of PM2.5 and PM10 aerosol in the Southern California air quality study. Atmos Environ 28:2061–2080. doi:10.1016/1352-2310(94)90474-X

Davidson CI, Phalen RF, Solomon PA (2005) Airborne particulate matter and human health: a review. Aerosol Sci Tech 39:737–749. doi:10.1080/02786820500191348

Ducret-Stich RE, Tsai MY, Ragettli MS, Ineichen A, Kuenzli N, Phuleria HC (2013) Role of highway traffic on spatial and temporal distributions of air pollutants in a Swiss Alpine valley. Sci Total Environ. doi:10.1016/j.scitotenv.2013.03.065

e-CFR: Title 40: Protection of environment; part 136-guidelines establishing test procedures for the analysis of pollutants [WWW Document] (2012). URL http://www.ecfr.gov/cgi-bin/text-idx?c=ecfr&SID=4310ba4cbc37140550f957fc4aab5841&rgn=div5&view=text&node=40:24.0.1.1.1&idno=40#40:24.0.1.1.1.0.1.8.2

Gehrig R, Hill M, Imhof D, Weingartner E, Baltensperger U (2004) Separate determination of PM10 emission factors of road traffic for tailpipe emissions and emissions from abrasion and resuspension processes. Int J Environ Pollut 22:312–325

Gehrig R, Hill M, Lienemann P, Zwicky CN, Bukowiecki N, Weingartner E, Baltensperger U, Buchmann B (2007) Contribution of railway traffic to local PM10 concentrations in Switzerland. Atmos Environ 41:923–933. doi:10.1016/j.atmosenv.2006.09.021

Gianini MFD, Fischer A, Gehrig R, Ulrich A, Wichser A, Piot C, Besombes J-L, Hueglin C (2012a) Comparative source apportionment of PM10 in Switzerland for 2008/2009 and 1998/1999 by positive matrix factorisation. Atmos Environ 54:149–158. doi:10.1016/j.atmosenv.2012.02.036

Gianini MFD, Gehrig R, Fischer A, Ulrich A, Wichser A, Hueglin C (2012b) Chemical composition of PM10 in Switzerland: an analysis for 2008/2009 and changes since 1998/1999. Atmos Environ 54:97–106. doi:10.1016/j.atmosenv.2012.02.037

Godoy MLDP, Godoy JM, Artaxo P (2005) Aerosol source apportionment around a large coal fired power plant—thermoelectric complex Jorge Lacerda, Santa Catarina, Brazil. Atmos Environ 39:5307–5324. doi:10.1016/j.atmosenv.2005.05.033

Hazenkamp-von Arx MH, Schindler C, Ragettli M, Künzli N, Braun-Fahrländer C, Liu L-J (2011) Impacts of highway traffic exhaust in alpine valleys on the respiratory health in adults: a cross-sectional study. Environ Health 10:13. doi:10.1186/1476-069X-10-13

Health Effects Institute (2010) HEI panel on the health effects of traffic-related air pollution. Traffic-related air pollution: a critical review of the literature on emissions, exposure, and health effects. Health Effects Institute, Boston

Hopke PK (2003) Recent developments in receptor modeling. J Chemometr 17:255–265. doi:10.1002/cem.796

Hueglin C, Gehrig R, Baltensperger U, Gysel M, Monn C, Vonmont H (2005) Chemical characterisation of PM2.5, PM10 and coarse particles at urban, near-city and rural sites in Switzerland. Atmos Environ 39:637–651. doi:10.1016/j.atmosenv.2004.10.027

Jordan TB, Seen AJ, Jacobsen GE (2006) Levoglucosan as an atmospheric tracer for woodsmoke. Atmos Environ 40:5316–5321. doi:10.1016/j.atmosenv.2006.03.023

Karanasiou A, Moreno N, Moreno T, Viana M, De Leeuw F, Querol X (2012) Health effects from Sahara dust episodes in Europe: literature review and research gaps. Environ Int 47:107–114. doi:10.1016/j.envint.2012.06.012

Khalil MA, Rasmussen R (2003) Tracers of wood smoke. Atmos Environ 37:1211–1222. doi:10.1016/S1352-2310(02)01014-2

Kim E, Hopke PK (2005) Improving source apportionment of fine particles in the Eastern United States utilizing temperature-resolved carbon fractions. J Air Waste Manag 55:1456–1463. doi:10.1080/10473289.2005.10464748

Kim E, Hopke PK (2004) Source apportionment of fine particles in Washington, DC, utilizing temperature-resolved carbon fractions. J Air Waste Manag 54:773–785. doi:10.1080/10473289.2004.10470948

Kim E, Hopke PK, Edgerton ES (2003a) Source identification of Atlanta aerosol by positive matrix factorization. J Air Waste Manag 53:731–739. doi:10.1080/10473289.2003.10466209

Kim E, Hopke PK, Paatero P, Edgerton ES (2003b) Incorporation of parametric factors into multilinear receptor model studies of Atlanta aerosol. Atmos Environ 37:5009–5021. doi:10.1016/j.atmosenv.2003.08.035

Laumbach RJ, Kipen HM (2012) Respiratory health effects of air pollution: update on biomass smoke and traffic pollution. J Allergy Clin Immun 129:3–11. doi:10.1016/j.jaci.2011.11.021

Liu W, Wang Y, Russell A, Edgerton ES (2006) Enhanced source identification of southeast aerosols using temperature-resolved carbon fractions and gas phase components. Atmos Environ 40(2):445–466. doi:10.1016/j.atmosenv.2005.11.079

Lough GC, Christensen CG, Schauer JJ, Tortorelli J, Mani E, Lawson DR, Clark NN, Gabele PA (2007) Development of molecular marker source profiles for emissions from on-road gasoline and diesel vehicle fleets. J Air Waste Manag 57:1190–1199. doi:10.3155/1047-3289.57.10.1190

Miller-Schulze JP, Paulsen M, Toriba A, Tang N, Hayakawa K, Tamura K, Dong L, Zhang X, Simpson CD (2010) Exposures to particulate air pollution and nitro-polycyclic aromatic hydrocarbons among taxi drivers in Shenyang, China. Environ Sci Technol 44:216–221. doi:10.1021/es802392u

Naeher LP, Brauer M, Lipsett M, Zelikoff JT, Simpson CD, Koenig JQ, Smith KR (2007) Woodsmoke health effects: a review. Inhal Toxicol 19:67–106. doi:10.1080/08958370600985875

Norris G, Vedantham R, Wade K, Brown S, Prouty J, Foley C (2008) EPA positive matrix factorization (PMF) 3.0 fundamentals & user guide. Washington DC, USA

Paatero P (1997) Least squares formulation of robust non-negative factor analysis. Chemometr Intell Lab 37:23–35. doi:10.1016/S0169-7439(96)00044-5

Paatero P, Hopke PK (2003) Discarding or downweighting high-noise variables in factor analytic models. Anal Chim Acta 490:277–289. doi:10.1016/S0003-2670(02)01643-4

Paatero P, Hopke PK, Begum BA, Biswas SK (2005) A graphical diagnostic method for assessing the rotation in factor analytical models of atmospheric pollution. Atmos Environ 39:193–201. doi:10.1016/j.atmosenv.2004.08.018

Paatero P, Hopke PK, Song X-H, Ramadan Z (2002) Understanding and controlling rotations in factor analytic models. Chemometr Intell Lab 60:253–264. doi:10.1016/S0169-7439(01)00200-3

Paatero P, Tapper U (1994) Positive matrix factorization: a non-negative factor model with optimal utilization of error estimates of data values. Environmetrics 5:111–126. doi:10.1002/env.3170050203

Polissar AV, Hopke PK, Paatero P, Malm WC, Sisler JF (1998) Atmospheric aerosol over Alaska: 2. Elemental composition and sources. J Geophys Res 103:19045–19,057. doi:10.1029/98JD01212

Pope CA, Dockery DW (2006) Health effects of fine particulate air pollution: lines that connect. J Air Waste Manag 56:709–742. doi:10.1080/10473289.2006.10464485

Putaud J-P, Van Dingenen R, Alastuey A, Bauer H, Birmili W, Cyrys J et al (2010) A European aerosol phenomenology—3: physical and chemical characteristics of particulate matter from 60 rural, urban, and kerbside sites across Europe. Atmos Environ 44:1308–1320. doi:10.1016/j.atmosenv.2009.12.011

Reid JS, Koppmann R, Eck TF, Eleuterio DP (2005) A review of biomass burning emissions part II: intensive physical properties of biomass burning particles. Atmos Chem Phys 5:799–825

Ringuet J, Albinet A, Leoz-Garziandia E, Budzinski H, Villenave E (2012a) Reactivity of polycyclic aromatic compounds (PAHs, NPAHs and OPAHs) adsorbed on natural aerosol particles exposed to atmospheric oxidants. Atmos Environ 61:15–22. doi:10.1016/j.atmosenv.2012.07.025

Ringuet J, Leoz-Garziandia E, Budzinski H, Villenave E, Albinet A (2012b) Particle size distribution of nitrated and oxygenated polycyclic aromatic hydrocarbons (NPAHs and OPAHs) on traffic and suburban sites of a European megacity: Paris (France). Atmos Chem Phys 12:8877–8887. doi:10.5194/acp-12-8877-2012

Russell AG, Brunekreef B (2009) A focus on particulate matter and health. Environ Sci Technol 43:4620–4625. doi:10.1021/es9005459

Sandradewi J, Prévôt ASH, Szidat S, Perron N, Alfarra MR, Lanz VA, Weingartner E, Baltensperger U (2008) Using aerosol light absorption measurements for the quantitative determination of wood burning and traffic emission contributions to particulate matter. Environ Sci Technol 42:3316–3323. doi:10.1021/es702253m

Schauer C, Niessner R, Pöschl U (2003) Polycyclic aromatic hydrocarbons in urban air particulate matter: decadal and seasonal trends, chemical degradation, and sampling artifacts. Environ Sci Technol 37:2861–2868

Schauer JJ, Lough GC, Shafer MM, Christensen WF, Arndt MF, DeMinter JT, Park JS (2006) Characterization of metals emitted from motor vehicles. Res Rep Health Eff Inst 1–76; discussion 77–88

Scheepers PTJ, Martens MHJ, Velders DD, Fijneman P, Van Kerkhoven M, Noordhoek J, Bos RP (1995) 1-Nitropyrene as a marker for the mutagenicity of diesel exhaust-derived particulate matter in workplace atmospheres. Environ Mol Mutagen 25:134–147. doi:10.1002/em.2850250207

Seinfeld JH, Pandis SN (2006) Atmos Chem Phys: from air pollution to climate change. John Wiley & Sons, New York, NY

Simoneit BRT, Schauer JJ, Nolte CG, Oros DR, Elias VO, Fraser MP, Rogge WF, Cass GR (1999) Levoglucosan, a tracer for cellulose in biomass burning and atmospheric particles. Atmos Environ 33:173–182. doi:10.1016/S1352-2310(98)00145-9

Simpson CD, Dills RL, Katz BS, Kalman DA (2004) Determination of levoglucosan in atmospheric fine particulate matter. J Air Waste Manag 54:689–694. doi:10.1080/10473289.2004.10470945

Stanek LW, Sacks JD, Dutton SJ, Dubois J-JB (2011) Attributing health effects to apportioned components and sources of particulate matter: an evaluation of collective results. Atmos Environ 45:5655–5663. doi:10.1016/j.atmosenv.2011.07.023

Sweetman JA, Zielinska B, Atkinson R, Ramdahl T, Winer AM (1967) Pitts Jr. JN (1986) A possible formation pathway for the 2-nitrofluoranthene observed in ambient particulate organic matter. Atmos Environ 20:235–238. doi:10.1016/0004-6981(86)90230-1

Szidat S, Jenk TM, Synal H-A, Kalberer M, Wacker L, Hajdas I, Kasper-Giebl A, Baltensperger U (2006) Contributions of fossil fuel, biomass-burning, and biogenic emissions to carbonaceous aerosols in Zurich as traced by 14C. J Geophys Res 111, D07206. doi:10.1029/2005JD006590

Szidat S, Prévôt ASH, Sandradewi J, Alfarra MR, Synal H-A, Wacker L, Baltensperger U (2007) Dominant impact of residential wood burning on particulate matter in Alpine valleys during winter. Geophys Res Lett 34, L05820. doi:10.1029/2006GL028325

Thorpe A, Harrison RM (2008) Sources and properties of non-exhaust particulate matter from road traffic: a review. Sci Total Environ 400:270–282. doi:10.1016/j.scitotenv.2008.06.007

Turpin BJ, Lim H-J (2001) Species contributions to PM2.5 mass concentrations: revisiting common assumptions for estimating organic mass. Aerosol Sci Tech 35:602–610. doi:10.1080/02786820119445

US EPA (2009) Integrated science assessment for particulate matter (final report). U.S. Environmental Protection Agency, Washington DC, USA

Viana M, Kuhlbusch TAJ, Querol X, Alastuey A, Harrison RM, Hopke PK et al (2008) Source apportionment of particulate matter in Europe: a review of methods and results. J Aerosol Sci 39:827–849. doi:10.1016/j.jaerosci.2008.05.007

Wu C, Larson TV, Wu S, Williamson J, Westberg HH, Liu L-JS (2007) Source apportionment of PM2.5 and selected hazardous air pollutants in Seattle. Sci Total Environ 386:42–52. doi:10.1016/j.scitotenv.2007.07.042